IEEE Access
Multidisciplinary | Rapid Review | Open Access Journal

Received September 14, 2020, accepted September 28, 2020, date of publication October 6, 2020, date of current version October 20, 2020.

Digital Object Identifier 10.1109/ACCESS.2020.3029093

Tracking Capability and Detection Probability Assessment of Space-Based Automatic Identification System (AIS) From Equatorial and Polar Orbiting Satellites Constellation

WAHYUDI HASBI[1], (Senior Member, IEEE), AND KAMIRUL[2], (Member, IEEE)
[1]Satellite Technology Center, National Institute of Aeronautics and Space (LAPAN) Indonesia, Bogor 16310, Indonesia
[2]Satellite Control, Space and Atmospheric Observation, and Remote Sensing Office, National Institute of Aeronautics and Space (LAPAN), Biak 98118, Indonesia

Corresponding author: Wahyudi Hasbi (wahyudi.hasbi@lapan.go.id)

The publication of this work is funded by the Satellite Technology Center, the National Institute of Aeronautics and Space (LAPAN), Indonesia.

ABSTRACT Performance of LAPAN-A2 and LAPAN-A3 space-based Automatic Identification System (AIS) have been successfully assessed as the satellites operated at individual and two-satellites constellation modes. Since LAPAN-A2 and LAPAN-A3 respectively orbiting at 6° and 97° of inclination, they form a unique constellation; hence, assessment on AIS performance from this equatorial-polar constellation is unprecedented. The assessment is intended to measure both the system and receiver performance of space-based AIS. The measurement of system performance calculates the capability of a space-based AIS system in re-detecting a ship as it moves globally. This performance is used to analyze whether the satellite and its AIS payload are systematically well-configured, including its orbital properties, antenna placement, and receiver's ability. The measurement of receiver performance is aimed to analyze the receiver capability in detecting all existing ships transmitting the AIS messages. This performance is represented as the ratio between the number of ships detected by the space-based AIS receiver and an ideal AIS receiver. In our case, massive AIS messages collected by an integrated space-terrestrial AIS receiver network has been used as the benchmark. By using 31 days of the collected AIS dataset, operating the satellites as a constellation increases the system and receiver performance by a factor of 7.56% and 7.93%, respectively. The further result shows that the constellated AIS receiver performs excellently in the deep-sea regions, with the value of system performance ranging from 95% to 100%. Moreover, the receivers of constellation satellites overperformed the benchmark receiver on up to 61.84% of their full coverage. The main contribution of this research is to provide information related to the advantages of operating equatorial-polar AIS constellation regarding its in-orbit performance. The results could become a reference in developing a space-based maritime surveillance tool with excellent performance and frequent accesses in those regions.

INDEX TERMS LAPAN-A2, LAPAN-A3, space-based AIS, performance, satellite, orbit.

I. INTRODUCTION

Automatic Identification System (AIS) is an automatic tracking system used by ships and vessel traffic services (VTS) to perform data exchanging between the vessels to other vessels, coastal stations, and satellites [1], [2]. AIS reporting system allows ships to broadcast short fixed-length Time Division Multiple Access (TDMA) messages containing their voyage information. AIS information can be used in different applications, including dynamic tracking, collision avoidance system, pilot scheduling, and assist in navigation decisions [3]–[5]. Nowadays, the rapidly growing communications, networks, and information technologies lead the AIS to become a reliable component in

The associate editor coordinating the review of this manuscript and approving it for publication was Yuan Zhuang.

establishing navigational aid and safety information system globally [6], [7].

Initially, the AIS technology was designed to be used in terrestrial-based vessel monitoring applications with up to 40 nautical miles of visibility. However, due to the rapidly increasing demand for vessel monitoring, attaching an AIS receiver to a satellite, i.e., space-based AIS, is beneficial for gaining global vessel surveillance capability [8], [9]. Since the space-based AIS is capable of providing a large swath area (up to 15 million km^2 at 500 km of altitude), this system is the most suitable component for demonstrating maritime wide-area surveillance. As a comparison, due to the existence of curvature of the Earth, the line-of-sight for ship-to-ship communications is limited to only 40-60 km, depending on antenna height. This advantage has attracted government space agencies and private companies, including Indonesia, to equip their satellite with an AIS payload to gather vessel information from Low Earth Orbit (LEO) [10], [11].

As the largest archipelago country in the world, Indonesia consists of 5.8 million km^2 of water area or 75% of the entire region. This geographic advantage necessitates Indonesia to enhance its maritime surveillance capability in which can be achieved by implementing satellite-based AIS. Therefore, a pair of experimental Indonesian microsatellites carrying AIS payloads, LAPAN-A2 and LAPAN-A3, has been built and injected into LEO orbit in 2015 and 2016, respectively.

LAPAN-A2 and LAPAN-A3 are the second and the third generation microsatellites developed and operated by the Satellite Technology Center, Indonesian National Institute of Aeronautics and Space (LAPAN). LAPAN-A2, also known as LAPAN-ORARI (IO-86), has been launched on 28 September 2015 and placed in near-equatorial orbit with an inclination of 6° at 650 km of altitude. The most recent satellite, LAPAN-A3, also known as LAPAN-IPB, has been launched on 22 June 2016 and has been injected into polar sun-synchronous orbit (97° of inclination), 505 km above sea level. Based on those orbital properties, LAPAN-A2 and LAPAN-A3 microsatellites pass through the Indonesian region 14 and 4 times per day. In addition to the AIS payload, the LAPAN-A2 satellite was also equipped with a medium multispectral camera, Automatic Package Reporting System (APRS), and Voice Repeater (VR). For the LAPAN-A3, a hybrid fluxgate magnetometer, multispectral push-broom imager, digital matrix camera, and a video camera were also attached to demonstrate earth observation missions [12]–[15].

Each of the LAPAN-A2 and LAPAN-A3 AIS system consisted of a receiver and a monopole antenna using frequency point at 161.975 MHz and 162.025 MHz, the official frequencies promulgated by the ITU for the traditional AIS system [16]. Nowadays, each of these satellites can record about 13 thousand unique ships transmitting 2.5 million vessel messages per day [12]. Those collected messages have been widely used for a specific application such as illegal fishing detection, investigation of vessel destructing coral reefs, and provision of necessary data for maritime authorities in investigating piracy cases around the Indonesian sea. According to those contributions, the AIS datasets provided by LAPAN-A2 and LAPAN-A3 become a primary component in performing maritime surveillance, especially in Indonesian sea territory.

Due to the importance of LAPAN-A2 and LAPAN-A3 space-based AIS for maritime surveillance purposes, it is necessary to assess these satellites' in-orbit performance. The assessment is intended to measure the performance of respective satellites as they operated as an individual satellite and to analyze the impact of incorporating them as they operated simultaneously, forming equatorial-polar space-based AIS constellation. To represent the performance, in this work, we have employed two types of statistical analysis, tracking capability and detection probability.

The tracking capability is used to express the overall performance of a space-based AIS system, which can be influenced by several factors such as receiver capability and satellite orbit. This includes other factors related to the environment, e.g., signal interference and message collision. According to this definition, it is reasonable to denote the tracking capability as ''system performance'' as used in this paper. Technically, the tracking capability, i.e., system performance, can be obtained by calculating the probability of a particular space-based AIS system to re-detect an already detected ship as both of the satellite and the ship are moving globally after the first detection. This type of approach has already been introduced by Skauen in [17] to quantify the system performance of Norwegian space-based AIS. The idea behind this approach is that for an ideal AIS system, at least one of the AIS messages transmitted by a particular ship should be received by the space-based AIS as it crosses the ship's horizon. However, in the real case, due to the imperfect condition of one or more factors influencing the system performance, the absence of received messages might occur. Therefore, the system performance of a space-based AIS system can be estimated by comparing the total number of messages received by the space-based AIS to the total number of the satellite passing through the ship's horizon.

Since the system performance only represents the overall capability of a space-based AIS, in this work, we have also experimented with measuring the performance of space-based AIS sub-system, i.e., the receiver. The receiver performance has been quantified by involving another AIS dataset as a reference, and the result is represented as a detection probability. The detection probability is expressed as the ratio between the number of ships detected by a space-based AIS receiver and those recorded by an ideal AIS receiver [18]. In this work, we used a globally-collected AIS dataset provided by a company engaged in maritime data services as the ideal AIS source. This option is reasonable since this company has exploited a massive terrestrial receivers network combined with space-based AIS receivers to provide an extensive and nearly real-time AIS dataset. In this work, the resulted receiver performance was used as the complementary material for assessment purposes. By having the

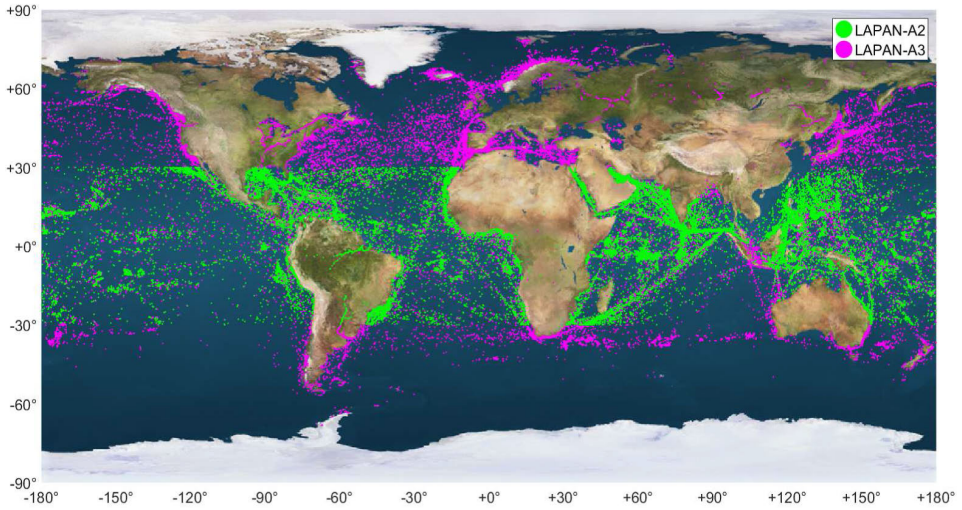

FIGURE 1. Static distribution of global vessels obtained by LAPAN-A2 (green dot) and LAPAN-A3 (purple dot) AIS receiver within 00.00 UT on 1 May 2019 to 23.59 on 31 May 2019.

information related to the receiver performance, one can predict other AIS sub-systems' performance. For example, suppose the system performance in a particular area is unsatisfactory, whereas the receiver performance is the opposite. In that case, the other factors apart from the receiver are responsible for the decline in the performance.

Finally, the results of this work are organized to produce information about the advantages of using equatorial-polar AIS constellation in terms of its in-orbit performance. Since this type of constellation can re-visit both equatorial and polar regions in a short period, the results presented could become a reference in developing a reliable space-based maritime surveillance tool with excellent performance and a high number of accesses both in equatorial and polar regions.

II. MATERIAL AND METHOD

A. AIS DATASET

In this work, we used three different AIS datasets. The first dataset consists of space-based AIS messages transmitted by the ships that existed at the equatorial region at approximately from $-30°$ to $+30°$ of latitude. This dataset was collected by the LAPAN-A2 AIS receiver from 00:00 UTC on 1 May 2019 to 23:58 UTC on 31 May 2019. Since the LAPAN-A2 satellite orbiting at near-equatorial orbit with 6° of inclination, it can monitor the maritime activity around the equatorial region, including Indonesia, 14 times per day.

The second dataset was gathered by polar-orbiting satellite, LAPAN-A3. This dataset was acquired from 00:00 UTC on 1 May 2019 to 23:59 UTC on 31 May 2019. As the LAPAN-A3 orbiting at 97° of inclination, it is capable of receiving AIS messages on the higher northern and southern latitudes compared to LAPAN-A2. In the present, together with LAPAN-A2, the LAPAN-A3 is continuously operated to provide global ship monitoring service having a high number of accesses both in the equatorial and polar regions.

The third dataset was recorded by an AIS network in which is the combination of terrestrial & space-based AIS receivers operated by a private company. We have received the complete version of this dataset acquired from 00:00 UTC on 1 May 2019 to 23:59 UTC on 31 May 2019. We treated this dataset as a benchmark in calculating the detection probability, i.e., receiver performance. Employing this dataset as the benchmark is reasonable since this dataset is the most comprehensive one compared to LAPAN-A2 and LAPAN-A3 datasets in terms of the number of collected messages and unique MMSIs (Maritime Mobile Service Identity). We used the term "benchmark dataset" to represent the dataset recorded by the AIS network for convenience.

TABLE 1. Comparison of the total number of unique ships and messages received by different AIS receivers over 31 days.

Name	AIS source	Number of unique ship	Number of messages
A2 dataset	LAPAN-A2	41,484	10,281,481
A3 dataset	LAPAN-A3	52,109	3,493,627
Benchmark dataset	AIS network (space & terrestrial)	481,355	817,123,179

Furthermore, the dataset produced by the LAPAN-A2 and LAPAN-A3, respectively, are denoted as the "A2 dataset" and "A3 dataset". For simplicity, the term "LAPAN datasets" is also used to represent both the A2 and A3 datasets. The complete comparison of these datasets over the given acquisition range (31 days) is provided in Table 1.

All of the available datasets provide information fields such as MMSI, timestamp, geographic position, speed, heading, and message type. Fig. 1 and Fig. 2, respectively, show the static distribution of unique ships identified by their MMSI detected by the satellites and terrestrial-based AIS in global coverage.

B. AIS DATA PRE-PROCESSING

This section is provided to give a detailed explanation related to AIS data pre-processing stages. Before calculating the

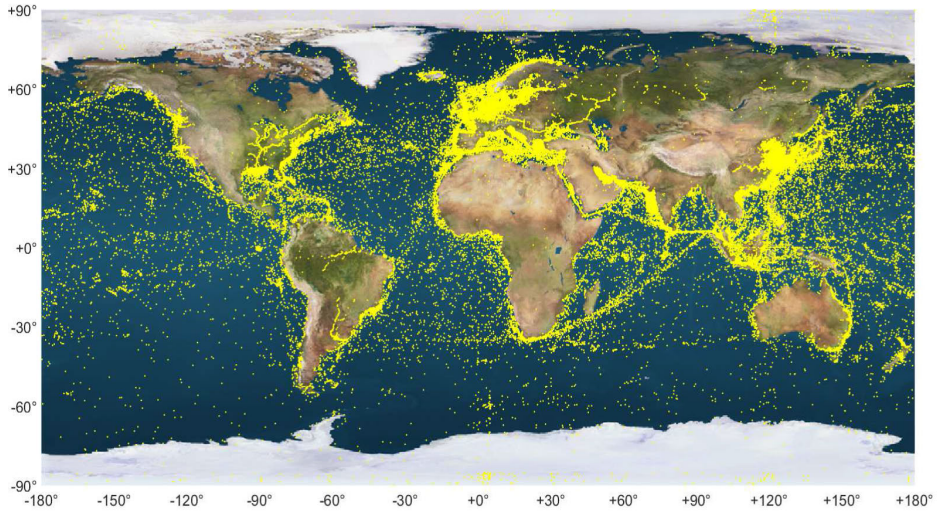

FIGURE 2. Static distribution of global vessels on benchmark dataset recorded by combined terrestrial & space-based AIS network within the time interval of 00.00 UT on 1 May 2019 to 23.59 on 31 May 2019.

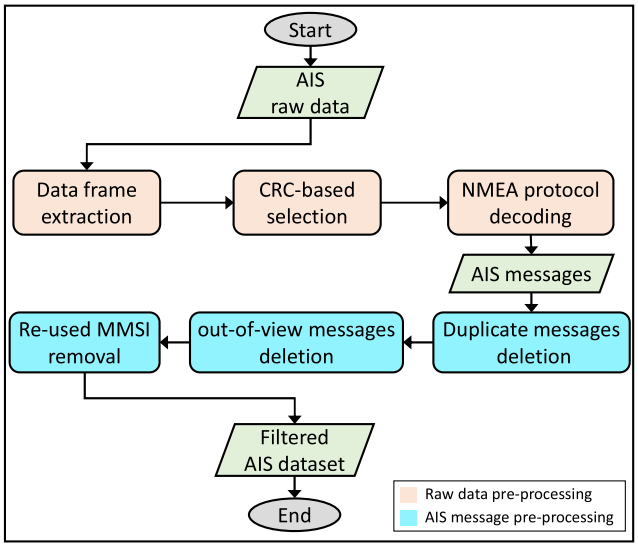

FIGURE 3. The chain used for pre-processing AIS raw data and AIS messages.

performances, all of the space-based AIS raw data is fed into a pre-processing chain to guarantee the resulted dataset free from unwanted noise and erroneous messages. As depicted in Fig. 3, the pre-processing chain consists of two main stages, i.e., raw data and AIS message pre-processing. For the sake of better understanding, we expanded the explanation of these stages into two respective sections.

1) RAW DATA PRE-PROCESSING

The raw data pre-processing stage is used to produce a dataset containing AIS messages from binary data gathered by the ground receivers. This type of pre-processing consists of three consecutive sub-stages as follows:

a) Firstly, a searching algorithm used to recognize the locations of desired AIS data frames is performed. Afterward, the frame extraction technique is applied based on those location identifiers. This step results in AIS data blocks containing ship-related parameter and Cyclic Redundancy Check (CRC) identifier. The CRC identifier holds the information related to frame quality, which can be used to remove noise-disturbed blocks.

b) Secondly, since the collected AIS raw data often suffer from unwanted noise and other artifacts, a data selection schema to remove noise-contaminated blocks must be applied. In this step, the selection process is made based on the CRC identifiers. The blocks of data marked by a specific CRC identifier representing the noise-contaminated state will be canceled out. Finally, an AIS dataset holding only noise-free data blocks will be resulted after passing through this step.

c) Lastly, to convert the raw data into an interpretable format, a decoding process need to be performed. This process is run by implementing the National Marine Electronics Association (NMEA) decoding protocol specifically designed for the respective LAPAN-A2 and LAPAN-A3 satellites. As a result, a dataset containing static and dynamic parameters of the ships is then resulted at the end of this step.

2) MESSAGE PRE-PROCESSING

Even though the dataset resulted from the raw data pre-processing chain is free from unwanted noise, this dataset could still suffer from unrepresentative AIS messages, e.g., duplicate messages, out-of-view messages, and messages transmitted by re-used MMSIs. In this work, we applied a sequence of filtering process to exclude all of those messages. The detail of AIS messages filtering is given as follows:

a) Firstly, we started from the most basic process, i.e., removing duplicate messages. This step is crucial since using duplicate messages is unnecessary and

leads to an incorrect final result caused by repetitive calculations. The duplicate messages might be found on the merged dataset as the combined LAPAN-A2 and LAPAN-A3 performance being assessed.

b) Secondly, to ensure dummy reporting location or out-of-view messages are not included in subsequent processing, we employed the SGP4 orbit propagator algorithm to remove those dummy messages. SGP4 was used to determine the coverage footprint of the respective satellite at a particular time. All messages reporting the positions outside of the satellite's coverage is then excluded from subsequent processing. Furthermore, since the benchmark dataset was used as the comparative dataset, this step is also applied to this dataset to provide a fair comparison between the LAPAN datasets and the benchmark dataset. It is not reasonable to compare the messages found in LAPAN datasets to those found in the benchmark dataset in a particular location while the satellites do not access such location. In other words, the comparative dataset for a particular satellite in a certain location consists only of the messages recorded by the AIS network during the visibility time of the respective satellite on that location.

c) Lastly, based on the fact that many MMSI identifiers are used by more than one ship, suspected re-used MMSI must be removed. The re-used MMSI identifier was identified and removed by calculating the speed required to move between two points based on timestamps and positions reported by the ships. In case the speed exceeds 60 knots, then MMSI is removed. The remaining MMSI identifiers are then used in the subsequent calculation.

The final product, filtered dataset free from unrepresentative AIS messages, is then used for performance measurement purposes.

C. CALCULATION OF SPACE-BASED AIS PERFORMANCE

In this paper, the tracking capability and detection probability terms represent the system and receiver performance of space-based AIS globally. Calculating the meter-resolution level's performance on the entire Earth's surface is very extensive; it is reasonable to carry out the calculation in a discrete manner. Hence, the global area was divided into grid cells to represent the tracking capability and detection probability of certain areas covered by those grid cells. In our work, a $2^\circ \times 2^\circ$ grid was used by default so that the Earth's surface is divided into 90×180 grids. A smaller or even larger grid size has not been investigated, but one must sensibly allow enough space for a large number of ships to fit on the grid.

1) SYSTEM PERFORMANCE

The system performance represented as tracking capability was determined by employing the method developed by Skauen presented in [17]. Tracking capability is defined as the probability of re-detecting an already detected ship as they move around the globe and are used to represent the performance of a space-based AIS system. The advantage of using this approach is that the calculation can be performed using only data recorded by the space-based AIS itself without involving any ground-truth dataset. In calculating the tracking capability, the following definitions are used:

- $N_{\text{det}}^{\text{MMSI}}(g)_{T_{\text{start}}}^{T_{\text{end}}}$: The number of space-based AIS accesses the grid cell g in which an MMSI was detected within a specified timeframe between T_{start} and T_{end}.
- $N_{\text{tot}}^{\text{acces}}(g)_{T_{\text{start}}}^{T_{\text{end}}}$: The total number of space-based AIS system accesses the grid cell g over the specified timeframe between T_{start} and T_{end}.

For the detection, a single message per access to an area is sufficient. Then, the tracking capability of a particular MMSI in a particular grid cell g, $TC_{MMSI}(g)$, can be quantified by using Eq. (1).

$$TC_{MMSI}(g) = \frac{N_{\text{det}}^{\text{MMSI}}(g)_{T_{\text{start}}}^{T_{\text{end}}}}{N_{\text{tot}}^{\text{acces}}(g)_{T_{\text{start}}}^{T_{\text{end}}}} \tag{1}$$

Afterward, the tracking capability, i.e., the re-detection probability for all MMSI on the grid cell g can be obtained by using Eq. (2),

$$PR(g) \sim TC(g) = \frac{\sum_{\text{MMSI}} TC_{\text{MMSI}}(g)}{N_{MMSI}(g)} \tag{2}$$

where $N_{MMSI}(g)$ refers to the total unique MMSI identifiers seen by the space-based AIS system.

In summary, to quantify the tracking capability as described in Eq. (1) and Eq. (2), the following steps must be performed:

- Calculate the access time of the space-based AIS system to every grid cell per pass over the specified timeframe using the SGP4 orbit propagator to obtain $N_{\text{tot}}^{\text{acces}}(g)_{T_{\text{start}}}^{T_{\text{end}}}$.
- Locate the position of each MMSI in grid representation by using available position information reported by the ships over the analysis timeframe in order to calculate $N_{\text{det}}^{\text{MMSI}}(g)_{T_{\text{start}}}^{T_{\text{end}}}$.
- Calculate the tracking capability, i.e., re-detection probability per MMSI by using Eq. (1), then quantify the re-detection probability for all MMSI per grid cell by employing Eq. (2).

As the space-based AIS system observes a grid cell multiple times over the specified timeframe, the resulted re-detection probability can be statistically accumulated. The accumulated result can be used to show the temporal evolution of system performance. The accumulated result can be calculated according to Eq. (3).

$$TC^{acc}(g) = 1 - \prod_{1}^{N_{\text{tot}}^{\text{acces}}(g)} (1 - TC(g)) \tag{3}$$

The $N_{\text{tot}}^{\text{acces}}(g)$ refers to the number of space-based AIS system accesses to a grid cell within the accumulation time in which

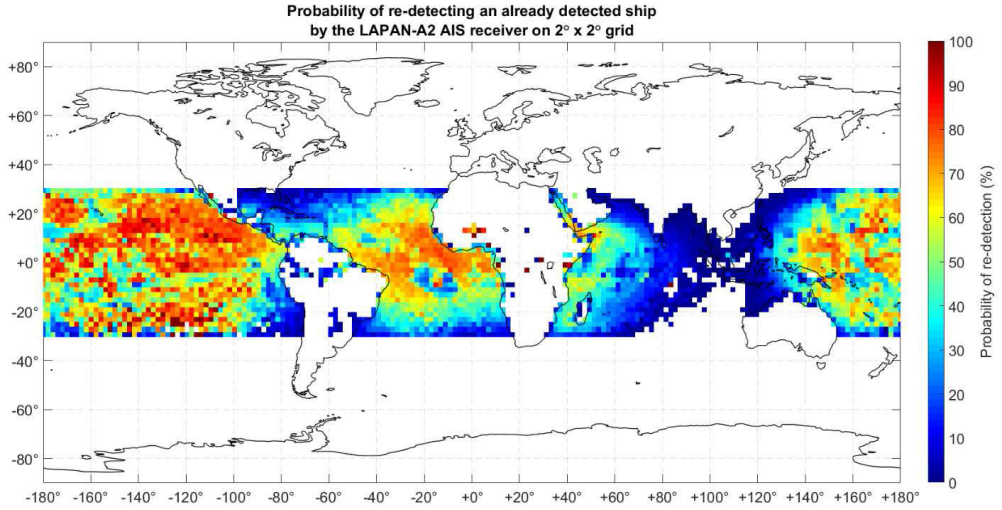

FIGURE 4. Distribution of global tracking capability using LAPAN-A2 space-based AIS receiver.

is also calculated using SGP4 propagator. The result $TC^{acc}(g)$ is then used to represent the average system performance within the accumulation time.

2) RECEIVER PERFORMANCE

The receiver performance was represented as detection probability. The detection probability can be obtained directly by comparing the number of ships detected by a space-based AIS receiver to the number of ships seen by the other AIS receiver in the same area over the same timeframe. In mathematical form, the equation used to calculate detection probability on a particular grid cell g can be expressed as:

$$DP(g) = \frac{N_{sat}(g)}{N_{bch}(g)} \tag{4}$$

where, $N_{sat}(g)$ and $N_{bch}(g)$ respectively, represent the total number of MMSIs seen by space-based AIS system and the total number of MMSIs collected by other AIS sources in the same grid cell during the same period.

A similar implementation of this approach can also be found in Li *et al.*'s work presented in [18]. In their work, the detection probability was used to quantify the performance of TianTuo-3 (TT3) satellite-based AIS. However, they only use two days continuously recorded dataset, which is insufficient to analyze the receiver's performance in a longer duration, mainly to cover the satellite's entire orbit.

III. RESULTS AND DISCUSSIONS

A. INDIVIDUAL SYSTEM PERFORMANCE OF LAPAN-A2 AND LAPAN-A3 SPACE-BASED AIS

This section describes the measurement results of individual system performance of LAPAN- A2 and LAPAN-A3 space-based AIS represented as tracking capability, i.e., re-detection probability.

The individual tracking capability of LAPAN-A2 and LAPAN-A3 space-based AIS, respectively, are presented in Fig. 4 and Fig. 5. In general, both results show that in the high traffic zones, such as East Asia, Western Europe, North America, and other economically active areas, the tracking capability is low, and even down to 0%. We have analyzed that this phenomenon is caused by a slight increase in the number of ships. As shown in Fig. 6, the number of ships per grid cell is exceptionally high in the high traffic zones. As a result, the chance of messages collision faced by the AIS receiver will increase as a massive amount of messages reach the AIS receiver simultaneously. Moreover, based on the AIS channels' signal environment map from space provided by [19], land-based interference sources are found near the high traffic zones. These sources were confirmed to have a contribution in degrading the system performance. However, in deep-sea regions with lower ship traffic density, such as the Pacific Ocean and South Atlantic Ocean, both the LAPAN-A2 and LAPAN-A3 AIS systems are in an excellent performance.

As the system performance represents the capability of an AIS system to track a particular ship during its movement, a high value of this performance can be influenced by three possible factors. Firstly, the amount of simultaneously received messages is still acceptable; hence, the space-based receiver experiences significantly less message collision. As a result, the possibility of a message to be successfully recorded by the satellite's onboard system will increase. Secondly, according to the AIS channels' signal environment map provided by [19], there is no source of interference found in the deep-sea regions. As a result, the probability of the AIS signal to reach the receiver is high. Thirdly, we have found and presented in Fig. 7 that the ships were actively moving at a higher speed in these regions than in high traffic zones. The higher the ships' speed, the shorter the reporting interval set by the ship AIS transceiver. For example, ships at anchor or not moving faster than 3 knots will automatically transmit their AIS signal every 3 minutes. Simultaneously, ships moving with speed larger than 3 knots will have reporting

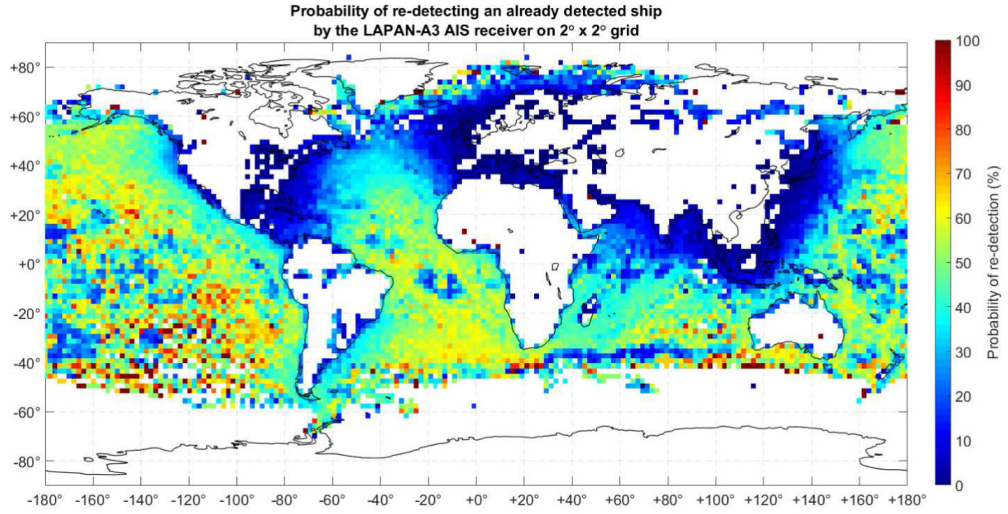

FIGURE 5. Distribution of global tracking capability using LAPAN-A3 space-based AIS receiver.

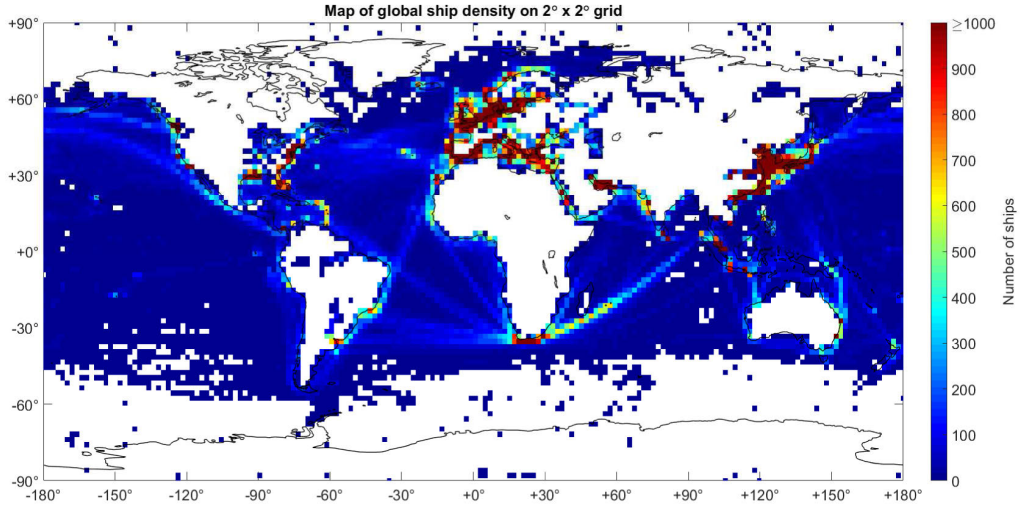

FIGURE 6. Global ship density map in 2°×2° grid generated using the benchmark dataset.

interval 2–10 seconds depending on their dynamic conditions. Therefore, as the averaged speed is relatively high in the deep-sea regions, shorter reporting interval will be set by the sailing ships in these regions. As a result, more messages will be transmitted during a satellite pass so that the probability of re-detecting a minimum one message per pass per ship will also increase. Since system performance represents the overall capability of a space-based AIS system, it can be inferred that this excellent performance could be influenced by at least one or all of those factors mentioned above.

It should be noted that the system performance presented this work has been estimated by involving a relatively small number of AIS data points since it resulted only from two constellated satellites. However, to implement a similar approach for an extremely large dataset, it is important to compress the ship trajectories for computational cost. One of the most successful approaches related to the ship trajectory compression has been demonstrated by Yu *et al.* [20]. In their work, massively parallel computation capabilities of the Graphics Processing Unit (GPU) have been employed to reduce the execution time of the Douglas-Peucker (DP) based trajectory compression algorithm. As a result, their approach is not only capable of reducing the amount of unnecessary AIS data points but also provides fast processing capability.

The averaged probability of re-detection of respective space-based AIS can be obtained by statistically accumulating the results in Fig. 4 and Fig. 5. The accumulated probability represents the re-detection probability's temporal evolution as the space-based AIS systems access a grid cell multiple times within the specified timeframe. This probability is then used to represent the averaged system performance within the specified time range. According to

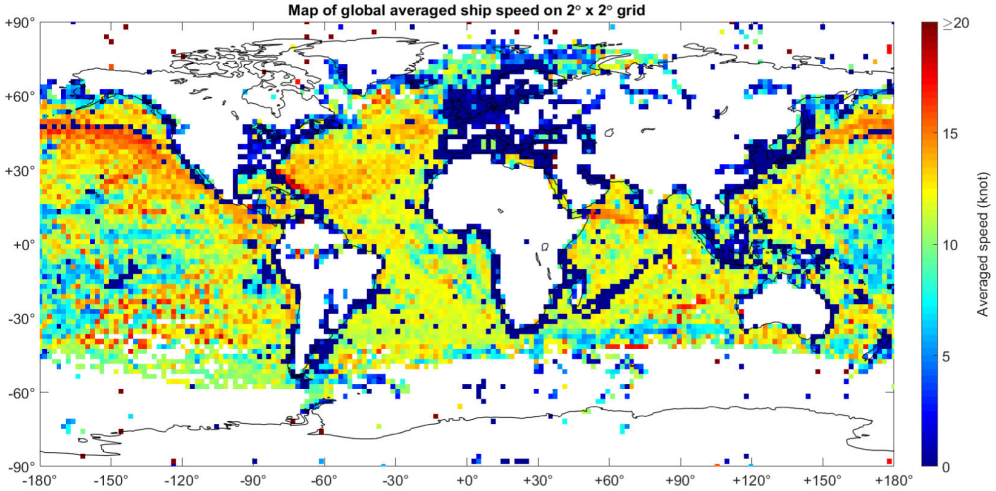

FIGURE 7. Averaged ship speed map in 2° × 2° grid generated using the benchmark dataset.

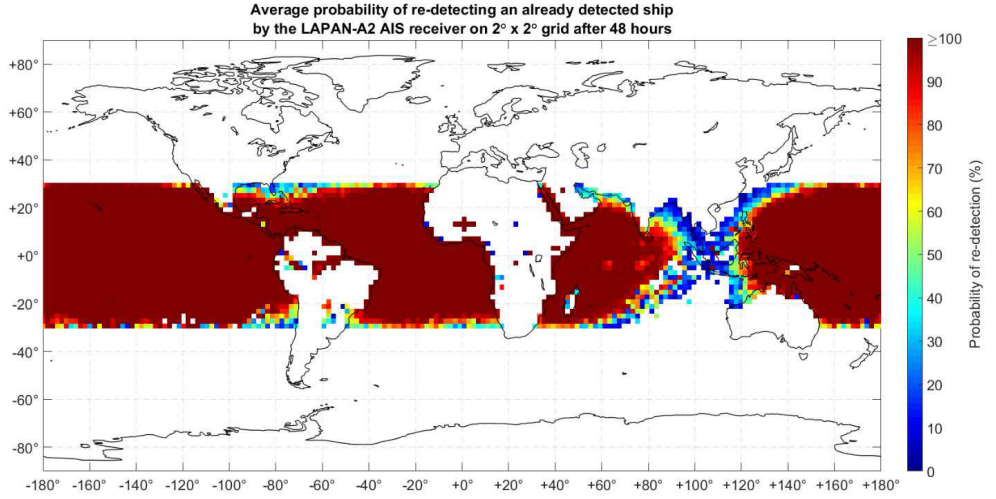

FIGURE 8. Statistically accumulated system performance of LAPAN-A2 space-based AIS receiver over 48 hours.

Fig. 8 and Fig. 9, the averaged system performance after 48 hours of in-orbit operation shows that both the LAPAN-A2 and LAPAN-A3 can establish their utility space-based AIS system as global maritime surveillance perfectly. The 48-hours of duration was chosen since, in our case, using the duration below this value is unable to produce a sufficient map showing the temporal evolution. Similar to the tracking capability pattern, it is found that both systems are excellent, resulting in 95%-100% of averaged performance in all deep-sea regions. However, in the Southeast Asia region, including the Gulf of Thailand and the Philippines Sea, the average performance of LAPAN-A2 is ranging from 0% to 50%. Furthermore, in areas populated by the high density of ships such as the Norwegian Sea, Mediterranean Sea, Black Sea, Baltic Sea, English Channel, South China Sea, and the East China Sea, the performance of LAPAN-A3 is also degrading, resulting in 0% to 70% of averaged performance.

Since the averaged system performance is directly derived from tracking capability, a low averaged performance experienced in high traffic zones, and the Southeast Asia region is suspected to be caused by the same factors as faced by the tracking capability, i.e., message collision and land-based signal interference. Even accumulated for 48 hours, there is no significant change in system performance in these zones. This result indicates that the message collision and signal interference are continuously happening and decreasing space-based AIS performance in these zones during the specified period. In contrast, as the averaged performance reaches the maximum values in the deep-sea regions, it can be inferred that during the specified period, both the ships and space-based AIS systems are respectively stable in transmitting and receiving the AIS signal. According to this result, it can be concluded that as individually operated, the LAPAN-A2 and LAPAN-A3 space-based AIS are reliable to

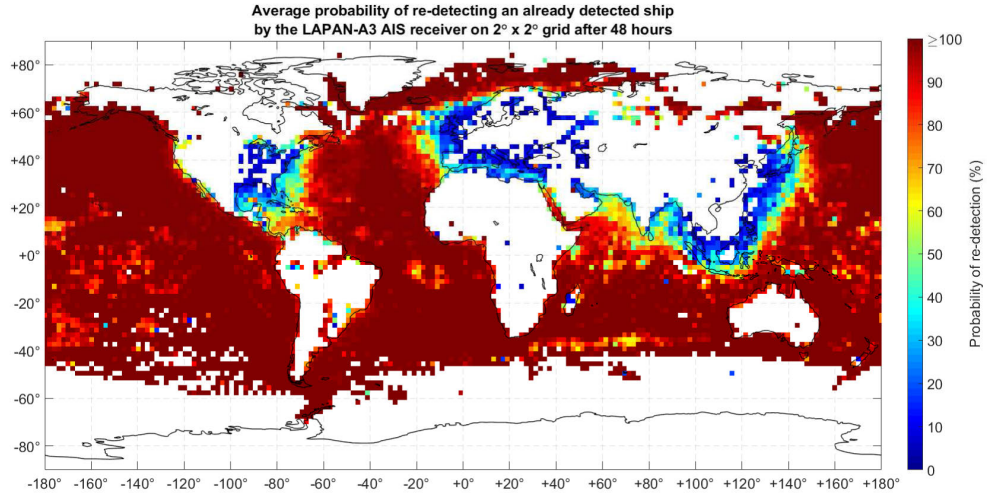

FIGURE 9. Statistically accumulated system performance of LAPAN-A3 space-based AIS receiver over 48 hours.

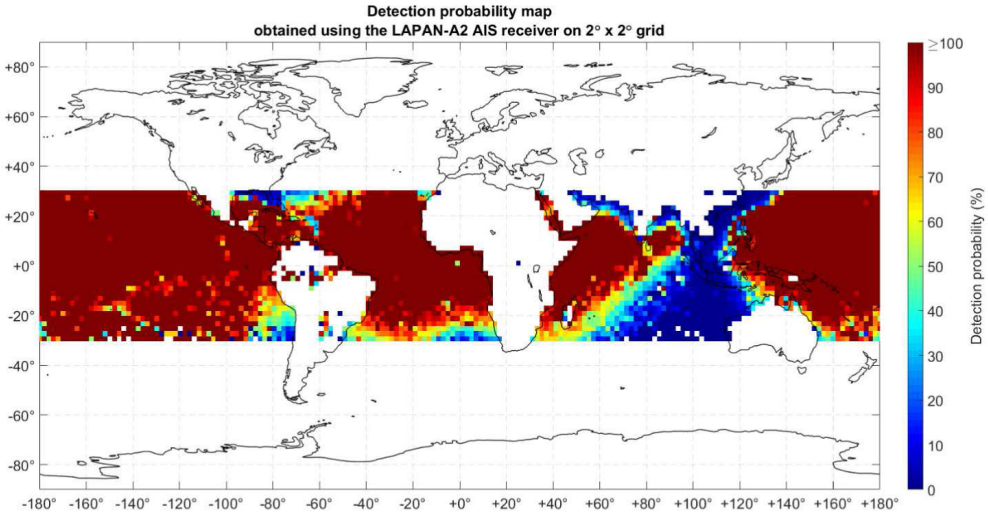

FIGURE 10. Global receiver performance obtained using LAPAN-A2 space-based AIS receiver.

be used in ship monitoring and tracking purposes in which are essential capabilities required to develop a maritime surveillance tool. However, there is an exception for LAPAN-A2 in the Indian Ocean as its system performance is relatively low in this region.

B. INDIVIDUAL RECEIVER PERFORMANCE OF LAPAN-A2 AND LAPAN-A3 SPACE-BASED AIS

In this section, the measurement results on individual LAPAN-A2 and LAPAN-A3 space-based AIS receivers performance are presented and discussed. The receiver performance was represented as detection probability in which can be obtained by comparing the number of ships detected by a space-based AIS receiver to those detected by a benchmark receiver.

In Fig. 10 and Fig. 11, the global receiver performance maps of LAPAN-A2 and LAPAN-A3 space-based receivers are presented.

For visualization purposes, the upper limit of performance shown in the maps is limited to 100%. According to Fig. 10 and Fig. 11, both of the LAPAN-A2 and LAPAN-A3 AIS receivers also experienced a low-performance in the high traffic zones similar to their system performance presented in Fig. 8 and Fig. 9. It is shown that the maximum receiver performance is about 60% with the lowest value near to 0% in the sea near the Europe mainland, Persian Gulf, East China Sea, South China Sea, and sea near the Southeast Asia region. Since the receiver performance represents a relative comparison between two different receivers, this low-performance value indicates that the LAPAN space-based AIS receiver is not as reliable as the benchmark receiver in high traffic zones. To explain why both LAPAN-AIS receivers experience a decline in performance in these regions, in Fig. 12, we provided the distribution of ship detected by different receiver types of the AIS network.

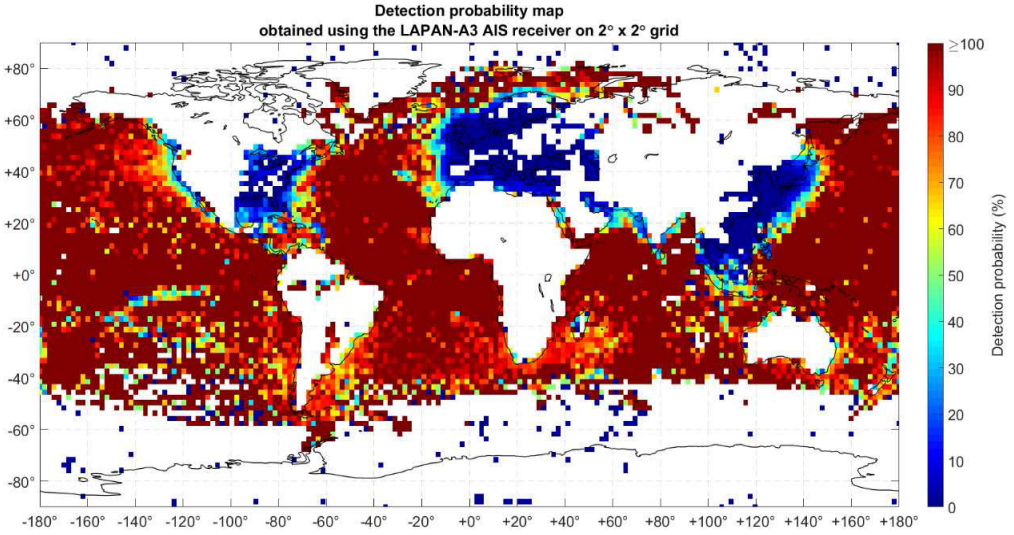

FIGURE 11. Global receiver performance obtained using LAPAN-A3 space-based AIS receiver.

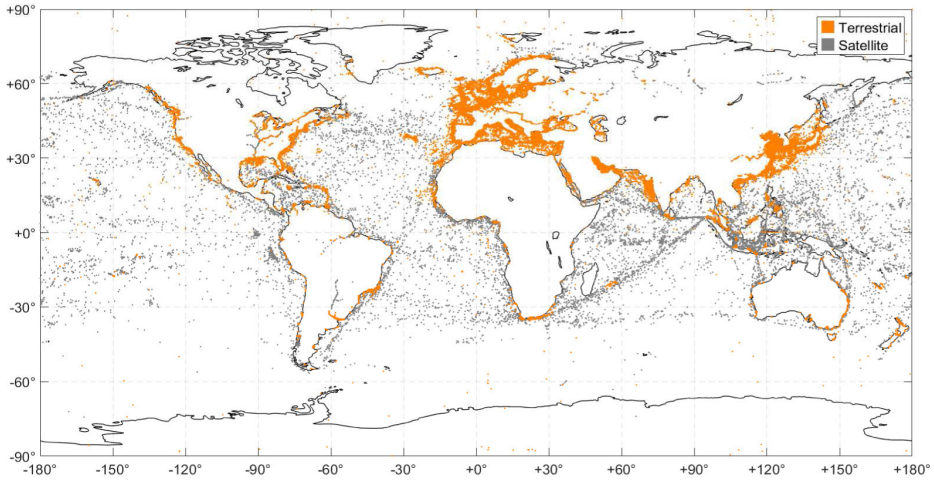

FIGURE 12. Distribution of ships detected by the different types of receivers of the AIS network. The orange-colored markers represent ships detected by the terrestrial receiver while the gray markers belong to the ships detected by the satellite receiver.

According to Fig. 12, it is shown that in the benchmark dataset, most of the ships found in high traffic zones were detected by the terrestrial receiver of the network. In contrast, in the area far from the land, the ships were mainly detected by the network's satellite-based receiver. This phenomenon indicates that the AIS network exploits and puts a high number of terrestrial-based receivers on the land near the high traffic zones. Moreover, this map also showed that the AIS network mainly operates its space-based receivers to accommodate the area's detection far from the land. Moreover, since a single terrestrial receiver's coverage is only up to 50 nautical miles, the number of ships covered by this receiver is not as much as the space-based AIS receiver. Therefore, the probability of the terrestrial-based receiver's message collision is lower than that of the LAPAN-A2 space-based receiver. This contradictive behavior between space-based and terrestrial-based receivers explains why the receiver performance is low in the high traffic zones.

Still based on Fig. 10 and Fig. 11, surprisingly, in the sparsely distributed regions far from the land, including the Pacific Ocean, Atlantic Ocean, the Indian Ocean, the individual performance of LAPAN-A2 and LAPAN-A3 receivers are excellent with the value ranging from 95% to 100%. Furthermore, in the extreme northern latitudes, the LAPAN-A3 receiver also demonstrates a satisfying performance varying from 60% to 100%. Since these regions are far from the land, based on Fig. 12, the AIS network operates only the space-based receivers. Hence, high receiver performance on these regions means that the individual LAPAN-A2 and LAPAN-A3 receivers can compete for the space-based AIS receiver used by the AIS network.

It should be noted that the upper limit of performance value shown in Fig. 10 and Fig. 11 are confined to 100%. It is found the values higher than 100%, representing that the LAPAN space-based AIS overperforms the AIS network.

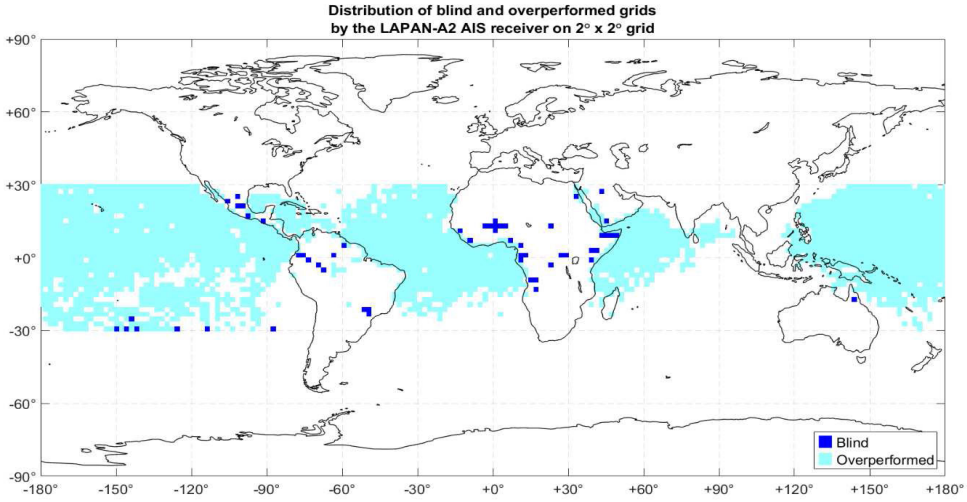

FIGURE 13. Global distribution of blind and overperformed grids obtained by LAPAN-A2 space-based AIS receiver.

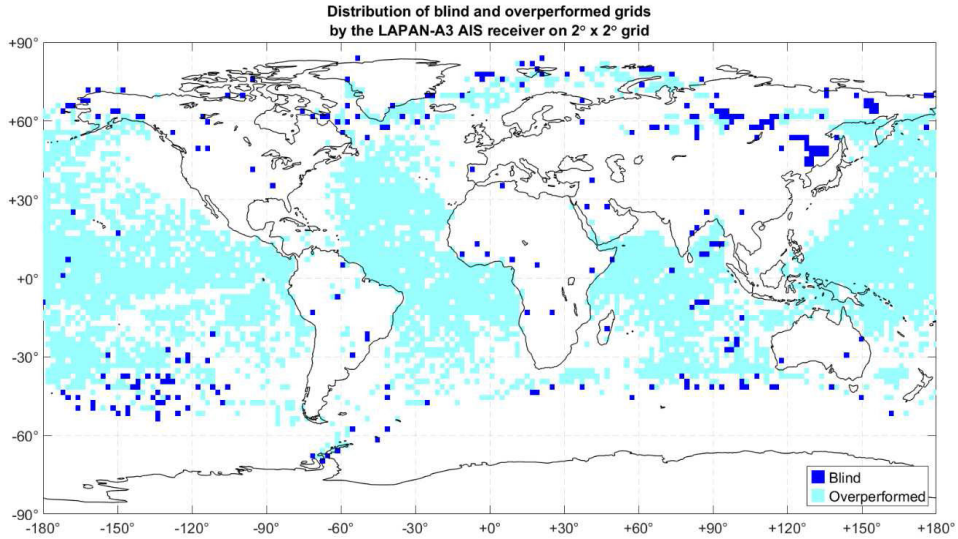

FIGURE 14. Global distribution of blind and overperformed grids obtained by LAPAN-A3 space-based AIS receiver.

To show the superiority of LAPAN AIS receivers over the AIS network receivers, in Fig. 13 and Fig. 14, we respectively provided the areas in which the LAPAN-A2 and LAPAN-A3 receivers detected more ships compared to the AIS network receivers. Fig. 13 and Fig. 14 consists of two categories of grids; ''blind'' and ''overperformed'' grid. The ''blind'' grid refers to a location in which none of the ships is found in the benchmark dataset but is existed in the LAPAN dataset. The other one, the ''overperformed'' grid, represents a location where one or more ships are detected in both datasets, but more ships are found on the LAPAN dataset.

We have calculated that in Fig. 13, respectively, 1.34% and 63.57% of the global coverage of LAPAN-A2 consisted of blind and overperformed grids. While in Fig. 14, the blind and overperformed grids take 3.30% and 47.85% of total grids covered by the LAPAN-A3 space-based AIS receiver. It is also shown that the blind and overperformed grids are mainly distributed in the deep-sea regions. Since the AIS network only has operated its space-based receivers in these regions, the existence of blind and overperformed grids proves that the LAPAN-A2 and LAPAN-A3 AIS receivers are not only having a satisfying performance in the deep-sea regions but also exceeds the performance of space-based receiver of the AIS network.

To deeply compare the capability of LAPAN space-based AIS and AIS network receiver, in Fig. 15, we have provided a snapshot of the number of unique ships detected by respective receivers.

We have verified that in some grids in the North Pacific Ocean near the Hawaiian Islands (Fig. 15 (A)), there is found 12 times larger of the number of ships in A2-dataset than that

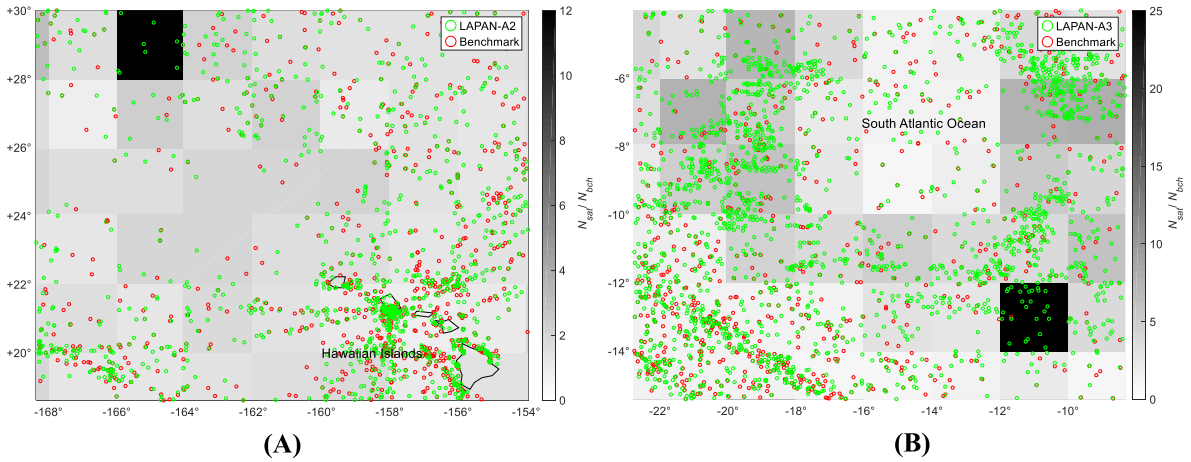

FIGURE 15. The maximum overperformed grid resulted by comparing the A2 dataset to the benchmark dataset; (B) similar result achieved using the A3 dataset.

found in the benchmark dataset. Moreover, in Fig. 15 (B), the highest performance of the LAPAN-A3 receiver was found in the South Atlantic Ocean with a value of 25. It should be noted that the calculation of receiver performance is based on the number of detected ships. Therefore, these results indicate that the LAPAN-AIS receivers are excellent in accumulating a high number of unique ships visiting a particular area. This capability complements their excellent tracking capability in the deep-sea regions, as previously discussed in Section III.A. Hence, it can be concluded that in the deep-sea regions, the LAPAN-A2 and LAPAN-A3 space-based AIS can be used to perform maritime surveillance activity capable of collecting a high number of ships and tracking them continuously.

Based on the results of the individual receiver performance of LAPAN-A2 and LAPAN-A3 space-based AIS, it can be seen that strategies to improve the detection probability are still required, especially in the high traffic zones. There is a possibility for currently orbiting satellites to improve detection probability by adjusting the monopole antenna orientation so that the AIS receiver's footprint in optimum performance. The term ''optimum'' in this context is related to a condition in which the footprint covers only a particular area so that the number of AIS transceivers covered by the receiver can be reduced. As a result, the probability of messages collision can be reduced, and the detection probability may increase accordingly [11].

C. SYSTEM AND RECEIVER PERFORMANCE OF CONSTELLATED LAPAN-A2 AND LAPAN-A3 SPACE-BASED AIS

In this section, assessment results on system and receiver performances of combined LAPAN-A2 and LAPAN-A3 space-based AIS are presented. The term ''combined'' is used to represent a situation in which the satellites are operated simultaneously as a constellation. For convenience, we used the term ''combined LAPAN-AIS'' to denote those combined LAPAN space-based AIS. Since the LAPAN-A2 orbiting at near-equatorial, the combination only affects the equatorial region's performance, from about -30° to +30° of latitude, the maximum latitude that can be covered by LAPAN-A2. Therefore, this region became the region of interest (ROI) in assessing both the system and receiver performance of combined LAPAN-AIS.

In Fig. 16, the global tracking capability map of combined LAPAN-AIS is shown. According to this map, in the Pacific Ocean and the Atlantic Ocean, the combined LAPAN-AIS capable of resulting satisfying system performance ranging from 70% to 100%. However, in the high traffic zones near South India, South China mainland, and waters nearby the Southeast Asia region, the low-performance is still experienced. This condition happened since both the individual LAPAN-A2 and LAPAN-A3 system performance are also low in these regions; hence, there is no significant improvement in performance even when the constellation scheme is applied.

As explained in Section III (A), three major factors, i.e., message collision, signal interference, and the variation of the speed of the ship globally, also influences the low-performance result in high traffic zones as well as high-performance result in deep-sea regions.

By specifically comparing the combined system performance map to the individual LAPAN-A2 performance in Fig. 4, it can be seen that the constellation schema is capable of increasing the low performance in the Indian Ocean as experienced by LAPAN-A2. This result indicates that the constellation schema can improve both the system performance and the number of passes in this region. As a comparison, by operating LAPAN-A2 and LAPAN-A3 satellites individually, the number of passes in a particular grid in the Indian Ocean are 14 and 4 times per day, respectively. As they operated together as constellated satellites, the number of passes becomes 18. Hence, this schema will benefit

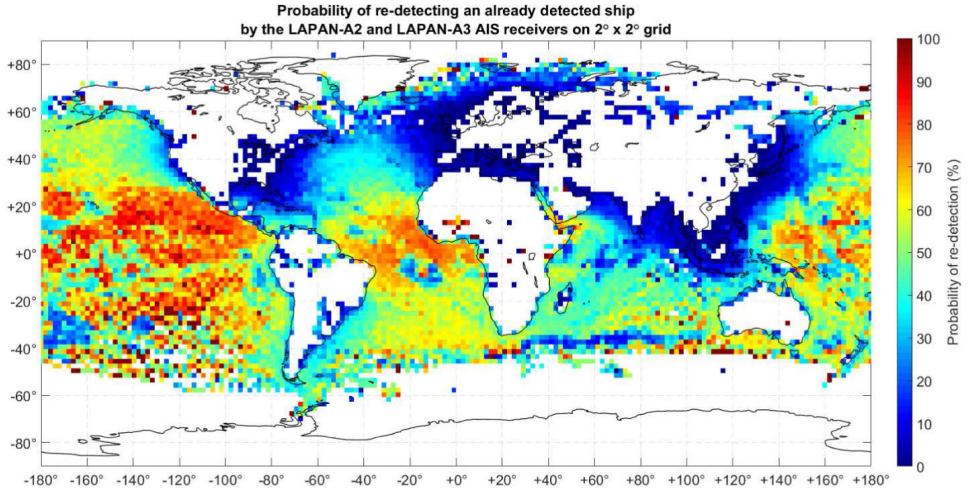

FIGURE 16. Distribution of global tracking capability obtained using combined LAPAN-AIS receivers.

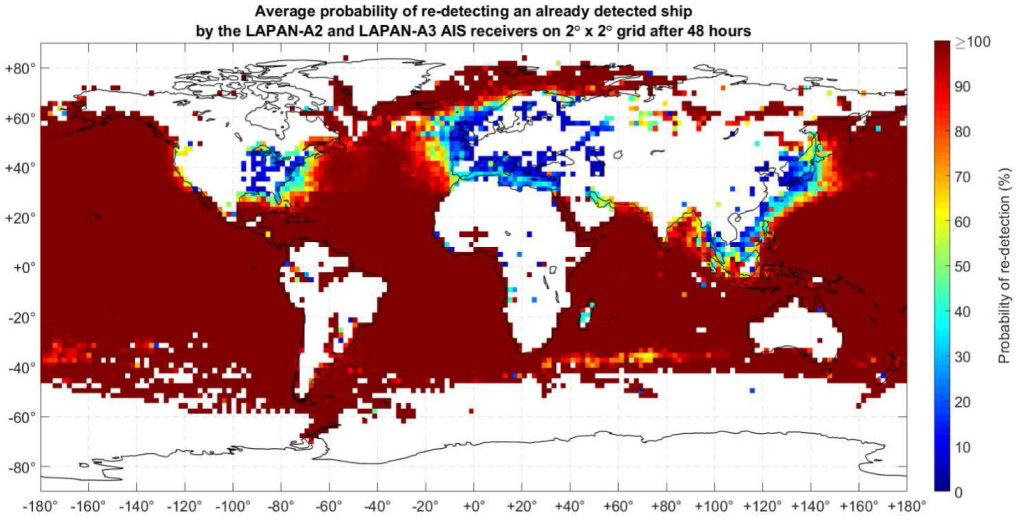

FIGURE 17. Statistically accumulated system performance obtained using combined LAPAN-AIS receivers.

one in developing a well-performed AIS system with a high number of accesses.

We have also compared the LAPAN-AIS combined system performance to those generated by combined Norwegian AISSat-1 and AISSat-2 space-based AIS reported in [17]. The complete comparison of the Norwegian AISSat constellation and LAPAN-AIS system performance in several locations is given in Table 2.

According to Table 2, there is found a close similarity of performance pattern between the Norwegian and LAPAN-AIS satellites. In the deep-sea regions such as the South Atlantic Ocean and the South Pacific Ocean, both the Norwegian and LAPAN-AIS demonstrate an excellent performance from 70% to 100%. However, in the high traffic zones, including the Gulf of Mexico, Mediterranean Sea, and the East China Sea, both of the system performance of the Norwegian and LAPAN-AIS satellites are drastically dropped between 0% to 20%. According to these results, it can be concluded that the Norwegian space-based AIS also faces the same problems as experienced by LAPAN satellites in these zones. Still referring to this table, it is also found that combined LAPAN-AIS overperforms the Norwegian AISSat constellation performance in some areas, i.e., the North Pacific Ocean and the Gulf of Guinea. Since the Norwegian AISSat constellation operating in polar orbit, it passes the deep oceanic regions about four times per day. It means that operating LAPAN-A2 and LAPAN-A3 as constellated satellites give an advantage in terms of the number of access provided and better system performance in those particular locations. Moreover, as the combined LAPAN-AIS provides a higher number of passes than that of the Norwegian AISSat constellation in the deep oceanic regions, the combined LAPAN-AIS is more suitable to be used as a ship monitoring tool in those regions.

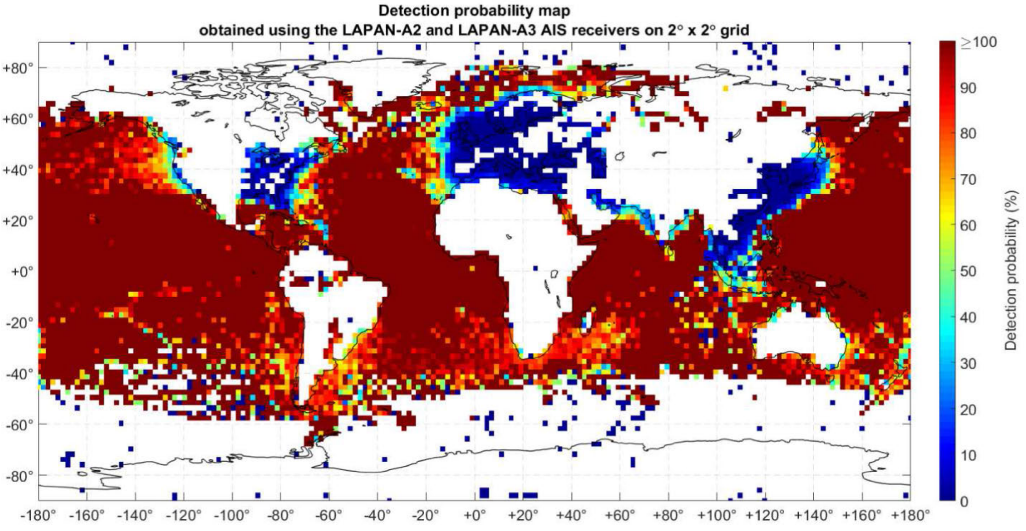

FIGURE 18. Global receiver performance was obtained using combined LAPAN-A2 and LAPAN-A3 space-based AIS receivers.

TABLE 2. Comparison of System Performance of The Norwegian AISSat Constellation and Combined LAPAN-AIS in Several Location.

Location	System performance (%)	
	Norwegian AISSat constellation	Combined LAPAN-AIS
South Atlantic Ocean and South Pacific Ocean	70 - 100	70 - 100
Gulf of Mexico, Mediterranean Sea, and the East China Sea	0 - 20	0 - 20
North Pacific Ocean and the Gulf of Guinea	60 - 80	70 - 100

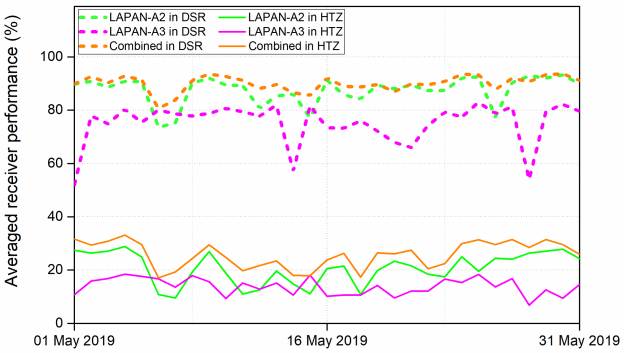

FIGURE 19. Comparison of daily receiver performance in high traffic zones (HTZ) and deep-sea regions (DSR).

The accumulated re-detection probability map of Fig. 16 representing the averaged system performance of combined LAPAN-AIS within a specific time range is shown in Fig. 17. Based on this map, it is clear that over 48 hours, the constellated satellites reach the best performance in almost all the deep-sea regions. This result is not surprising since the averaged individual performances of both satellites on the ROI also provide the same pattern, except in the Indian Ocean region. In that specific region, the individual performance of LAPAN-A2 is less compared to other regions. However, as the satellites are combined, the averaged performance in this region can be increased. According to this result, it can be concluded that the combined LAPAN-AIS is excellent to be used as a tracking system in all deep-sea regions, including the Indian Ocean.

By comparing the total number of unique ships found in the combined LAPAN-AIS dataset to those found in the benchmark dataset, combined LAPAN-AIS's receiver performance can be obtained. As presented in Fig. 18, the combined LAPAN-AIS receiver performance pattern resembles its system performance provided in Fig. 17. It is shown that in the deep-sea regions, the performance is almost perfect, with value ranging from 70% to 100%. Furthermore, in the waters near the Eastern United States, China mainland, and other economically active areas, similar to what was found in Fig. 17, declining in performance was also experienced by the combined LAPAN-AIS receivers. The receiver performance in these areas is ranging from 0% to 40%.

According to the result in Fig. 18, it can be concluded that even the constellation schema has been used, the combined receivers are unable to compete with the capability of massively-incorporated terrestrial-based receivers of the AIS network in the high traffic zones. However, compared to their individual performance, the constellation scheme is evidently capable of increasing the receiver performance in high traffic zones and deep-sea regions.

As provided in Fig. 19, in the deep-sea regions (denoted as "DSR"), the daily receiver performance increases to 80%-93% as the receivers combined. As a comparison, by operating only a single LAPAN-A3 receiver, a lower performance ranging from 52% to 82% is obtained. Moreover, in the high traffic zones (denoted as "HTZ"), the

TABLE 3. Comparison of results produced by individual and combined mode of LAPAN-AIS receivers in ROI.

Receivers	Globally-averaged system performance (%)	Globally-averaged receiver performance (%)	Blind grids ratio (%)	Overperformed grids ratio (%)
LAPAN-A2	43.80	80.77	1.34	63.57
LAPAN-A3	40.41	86.77	1.16	62.01
Combined LAPAN-AIS	49.67	91.70	1.48	61.84

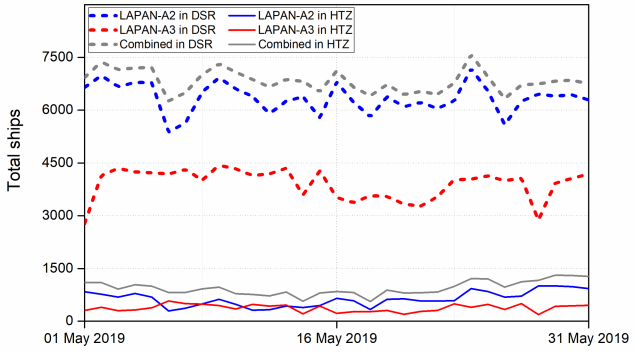

FIGURE 20. Comparison of daily total detected ships in high traffic zones (HTZ) and deep-sea regions (DSR).

constellation was also found to increase the averaged daily performance to the range of 17% - 33%. By operating a single LAPAN-A2 receiver, only 9% - 28% of performance has resulted. Simultaneously, the single receiver performance of LAPAN-A3 is the lowest in these zones, ranging from about 6% to 18%.

We have also compared the results in Fig. 19 to those resulting from Li *et al.*'s work presented in [18]. Li *et al.* have used a similar approach to assess the TianTuo-3 (TT3) space-based AIS receiver's performance. It is found that the average performance of TT3 in the near offshore regions is very close to those resulted from LAPAN-AIS receivers, ranging from 10% to 40%. However, in the sparsely distributed regions, this satellite's measured performance was relatively low compared to our result, with the value ranging from 40% to 70%. According to these results, based on daily receiver performance, the LAPAN-AIS receivers are better than TT3 in deep-sea regions.

In addition to daily receiver performance, in Fig. 20, we have also provided the detected ship's daily number. According to the plot in Fig. 20, the constellation schema is also found capable of increasing the receivers' capability in detecting unique ships.

It is confirmed that the total number of unique ships in high traffic zones and deep-sea regions can also be increased by incorporating the LAPAN-A2 and LAPAN-A3 space-based AIS receivers. In the high deep-sea regions, we have calculated that the combined receivers could improve the number of detected ships by up to 42.8% relative to LAPAN-A3. Simultaneously, 9.9% of improvement in the number of detected ships is also experienced as the combined result compared to those resulting from LAPAN-A2. Moreover, in the high traffic zones, the total number of ships collected by combined receivers is about 33.1% and 60.3% higher than those collected by single LAPAN-A2 and LAPAN-A3 receivers, respectively.

Last but not least, still based on Fig. 20, there is also found an interesting result. Even the number of ships existing in high traffic zones is slightly higher than that of the deep-sea regions (according to global ship density map in Fig. 6), an inverse phenomenon of performance is experienced by LAPAN-AIS receivers. This result reinforces the fact that the probability of message collisions in the high traffic zones is higher than that of deep-sea regions.

To summarize the comparison of results produced by operating LAPAN-AIS as single and as a constellation, in Table 3, we provided the globally-averaged performance, including the ratio of blind and overperformed grids. According to Table 3, it is confirmed that by operating the satellites simultaneously, the averaged system performance increase by 5.87% and 9.26% compared to the individual performance of LAPAN-A2 and LAPAN-A3, respectively. Moreover, it is also found that this strategy is also capable of improving the averaged receiver performance of about 10.93% and 4.93% compared to using individual LAPAN-A2 and LAPAN-A3 receiver, respectively. However, there is no significant improvement in the ratio of blind and overperformed grids as the satellites combined. This condition happened since the blind or overperformed grids found in individual satellites may decrease as a more significant number of ships in the benchmark dataset are also used in combined mode.

Finally, in addition to the improvement in the performance of space-based AIS, an alternative benefit of combining two or more satellites as a constellation is that one could increase the satellite's duration of observation as their footprints are sometimes overlapping. This increment also could decrease the period without satellite's visibility of an area. According to these facts, the constellation schema allows maritime monitoring more frequently in a longer observation duration.

IV. CONCLUSION

In this paper, a performance assessment on AIS receivers mounted on uniquely-constellated equatorial-polar satellites, LAPAN-A2 and LAPAN-A3, has been successfully conducted. The assessment is intended to analyze both the satellites' system and receiver performance as they are working in individual and constellated operation mode.

The measurement of system performance involves a calculation to determine the capability of a space-based AIS system in re-detecting an already detected ship. The

calculation used only the AIS dataset collected by the respective satellites as the input. The system performance is used to analyze whether the satellite and its AIS payload are systematically well-configured, including their orbital plane and altitude, antenna placement, and the receiver's ability to handle signal interference. As the in-orbit configuration of the space-based AIS system could change periodically, and a ship is probably moving globally to different environments, there is a possibility that the space-based AIS system does not detect the ship during a pass. Therefore, the system performance can be obtained by comparing the number of times the ship detected by the space-based AIS system to the number times the satellite crosses the ship's horizon. The receiver performance is represented as detection probability in which can be obtained by comparing the number of ships detected by the space-based AIS receiver to those detected by an ideal AIS receiver. An extensive dataset gathered by a combined space & terrestrial-based AIS receiver network has been used as the comparative dataset in our work. The assessment of receiver performance is very important to analyze whether the existing AIS receiver is already working as expected.

By using 31 days of continuously collected AIS datasets, it is found that the receiver performance of constellated LAPAN-A2 and LAPAN-A3 space-based AIS increases to a value of 91.70%. This value is relatively larger than those achieved by operating the LAPAN-A2 and LAPAN-A3 individually, resulting in 80.77% and 86.77% of performance, respectively. Based on the calculation, it is confirmed that the constellation schema is also capable of increasing the system performance to a value of 49.67%. As a comparison, the system performance values of LAPAN-A2 and LAPAN-A3 as they operated individually are 43.80% and 40.41%, respectively.

Further results also show that in the deep-sea regions, the constellated satellites demonstrate an excellent receiver performance with the value ranging from 95% to 100%. Moreover, during the same period of time, the LAPAN-A2 and LAPAN-A3 receivers overperform the AIS receiver network in terms of the total number of detected ships on up to 63.57% of their global coverage. Based on these results, it can be concluded that simultaneously operating equatorial-polar space-based AIS constellation is not only capable of providing a higher number of visiting time on respective regions but also increasing the system and receiver performance. Therefore, this type of AIS constellation schema is suitable to be implemented as a well-performed maritime surveillance tool capable of giving frequent accesses in both equatorial and polar regions.

ACKNOWLEDGMENT

The authors gratefully thank the Satellite Technology Center, the National Institute of Aeronautics & Space (LAPAN), Indonesia, for providing necessary space-based AIS datasets and funding the publication. Special thanks are also addressed to the PT. CLS Argos Indonesia for providing some of the comparative AIS datasets.

REFERENCES

[1] F. Lázaro, R. Raulefs, W. Wang, F. Clazzer, and S. Plass, "VHF data exchange system (VDES): An enabling technology for maritime communications," *CEAS Space J.*, vol. 11, no. 1, pp. 55–63, Mar. 2019, doi: 10.1007/s12567-018-0214-8.

[2] C. Yang, Q. Hu, X. Tu, and J. Geng, "An integrated vessel tracking system by using AIS, Inmarsat and China Beidou navigation satellite system," *Navig. Syst. Simulators*, vol. 6, no. 2, pp. 43–46, 2011, doi: 10.1201/b11343-8.

[3] Z. Pietrzykowski, P. Borkowski, and P. Wołejsza, "NAVDEC—Navigational decision suport system on a sea-going vessel," *Zeszyty Naukowe/Akademia Morska w Szczecinie*, vol. 30, no. 102, pp. 102–108, 2012.

[4] A. Felski, K. Jaskólski, and P. Banyš, "Comprehensive assessment of automatic identification system (AIS) data application to anti-collision manoeuvring," *J. Navigat.*, vol. 68, no. 4, pp. 697–717, Jul. 2015, doi: 10.1017/S0373463314000897.

[5] Q. Hu, L. Xu, and X. Cheng, "A CORS-based differential correction approach for AIS mobile stations," *Sensors*, vol. 18, no. 11, p. 3626, Oct. 2018, doi: 10.3390/s18113626.

[6] Z. Tian, F. Liu, Z. Li, R. Malekian, and Y. Xie, "The development of key technologies in applications of vessels connected to the Internet," *Symmetry*, vol. 9, no. 10, p. 211, Oct. 2017, doi: 10.3390/sym9100211.

[7] E. Tu, G. Zhang, L. Rachmawati, E. Rajabally, and G.-B. Huang, "Exploiting AIS data for intelligent maritime navigation: A comprehensive survey from data to methodology," *IEEE Trans. Intell. Transp. Syst.*, vol. 19, no. 5, pp. 1559–1582, May 2018, doi: 10.1109/TITS.2017.2724551.

[8] A. Harchowdhury, B. K. Sarkar, K. Bandyopadhyay, and A. Bhattacharya, "Generalized mechanism of SOTDMA and probability of reception for satellite-based AIS," in *Proc. 5th Int. Conf. Comput. Devices Commun. (CODEC)*, Dec. 2012, pp. 1–4, doi: 10.1109/CODEC.2012.6509332.

[9] T. Eriksen, A. N. Skauen, B. Narheim, O. Helleren, O. Olsen, and R. B. Olsen, "Tracking ship traffic with space-based AIS: Experience gained in first months of operations," in *Proc. Int. WaterSide Secur. Conf.*, Nov. 2010, pp. 1–8, doi: 10.1109/WSSC.2010.5730241.

[10] S. Plass, R. Poehlmann, R. Hermenier, and A. Dammann, "Global maritime surveillance by airliner-based AIS detection: Preliminary analysis," *J. Navigat.*, vol. 68, no. 6, pp. 1195–1209, Nov. 2015, doi: 10.1017/S0373463315000314.

[11] W. Hasbi, Kamirul, M. Mukhayadi, and U. Renner, "The impact of space-based AIS antenna orientation on in-orbit AIS detection performance," *Appl. Sci.*, vol. 9, no. 16, p. 3319, Aug. 2019, doi: 10.3390/app9163319.

[12] M. Mukhayadi, A. Karim, W. Hasbi, and R. Permala, "Designing a constellation for ais mission based on data acquisition of lapan-a2 and lapan-a3 satellites," *Telkomnika (Telecommun. Comput. Electron. Control.*, vol. 17, no. 4, pp. 1774–1784, 2019, doi: 10.12928/telkomnika.v17i4.12048.

[13] P. R. Hakim, A. H. Syafrudin, and S. Salaswati, "Analysis of radiometric calibration on matrix imager of LAPAN-A3 satellite payload," in *Proc. IEEE Int. Conf. Aerosp. Electron. Remote Sens. Technol. (ICARES)*, Dec. 2015, pp. 1–7, doi: 10.1109/ICARES.2015.7429831.

[14] W. Hasbi, "LAPAN-A2 (IO-86) satellite roles in natural disaster in Indonesia," in *Proc. 70th Int. Astron. Congr. (IAC)*, Washington, DC, USA, 2019.

[15] R. H. Triharjanto, H. Bangkit, and M. A. Saifudin, "Development of space-based magnetic activities measurement mission in LAPAN' s," in *Proc. 2nd Symp. Microsatellites Remote Sens.*, Aug. 2014, pp. 1–7, doi: 10.13140/2.1.2579.3920.

[16] *Technical Characteristics For A Universal Shipborne Automatic Operational Characteristics of a Universal Shipborne AIS Using TDMA Techniques in the VHF Maritime Mobile Band*, Int. Telecommun. Union, Geneva, Switzerland, 1998, pp. 1–44.

[17] A. N. Skauen, "Quantifying the tracking capability of space-based AIS systems," *Adv. Space Res.*, vol. 57, no. 2, pp. 527–542, Jan. 2016, doi: 10.1016/j.asr.2015.11.028.

[18] S. Li, L. Chen, X. Chen, Y. Zhao, and L. Yang, "Statistical analysis of the detection probability of the TianTuo-3 space-based AIS," *J. Navigat.*, vol. 71, no. 2, pp. 467–481, Mar. 2018, doi: 10.1017/S0373463317000649.

[19] A. N. Skauen and Ø. Olsen, "Signal environment mapping of the automatic identification system frequencies from space," *Adv. Space Res.*, vol. 57, no. 3, pp. 725–741, Feb. 2016, doi: 10.1016/j.asr.2015.12.002.

[20] Y. Huang, Y. Li, Z. Zhang, and R. W. Liu, "GPU-accelerated compression and visualization of large-scale vessel trajectories in maritime IoT industries," *IEEE Internet Things J.*, early access, Apr. 21, 2020, doi: 10.1109/jiot.2020.2989398.

WAHYUDI HASBI (Senior Member, IEEE) received the bachelor's degree in physics from Hasanuddin University, in 2000, and the master's degree in computer science from IPB University, Indonesia, in 2011. He is currently a Senior Researcher and Coordinator/Head of Dissemination Division, Satellite Technology Center, National Institute for Aeronautics and Space (LAPAN), Indonesia. He is currently pursuing the Ph.D. degree with the Institut für Luft-und Raumfahrt, Technische Universität Berlin, in 2020. He was involved as a System and Chief Engineer in microsatellite projects in Indonesia, including LAPAN-TUBSAT, LAPAN-A2/LAPAN-ORARI, and LAPAN-A3/IPB. In 2016, he received a prestigious medal award of Satyalancana Wirakarya (''Role Model Medal'') from the President of Republic Indonesia, which was specially awarded for ''Outstanding Dedication in Satellite Design and Development and Became A Role Model in The Satellite Technology Development to The Country.'' He is a Senior Member of the IEEE Aerospace & Electronic Systems Society (IEEE-AESS), Geoscience and Remote Sensing Society (IEEE-GRSS), and also the Technology and Engineering Management Society (IEEE-TEMS). He served as a Vice-Chair of the IEEE Indonesia Section, from 2017 to 2019. He was elected as an IEEE Indonesia Section Chair-Elect for 2021. He actively involves in research and publishes papers related to the field of satellite technology.

KAMIRUL (Member, IEEE) received the B.S. degree in physics from Tanjungpura University, Indonesia, in 2014, and the M.S. degree in physics from the Institut Teknologi Bandung, Indonesia, in 2017. He is currently working as an Engineer with the Indonesian National Institute of Aeronautics and Space (LAPAN). His research interest includes the AI-based detection system, medical imaging, parallel computing, and satellite image processing. He was an awardee of the Indonesia Endowment Fund for Education Scholarship (LPDP) from the Indonesian Ministry of Finance in 2015.